Lightning-Initiation Locations as a Remote Sensing Tool of Large Thunderstorm Electric Field Vectors

CHRISTOPHER MAGGIO, LEE COLEMAN, THOMAS MARSHALL, AND MARIBETH STOLZENBURG

Department of Physics and Astronomy, University of Mississippi, University, Mississippi

MARK STANLEY

Los Alamos National Laboratory, Los Alamos, New Mexico

TIMOTHY HAMLIN, PAUL KREHBIEL, WILLIAM RISON, AND RON THOMAS

Geophysical Research Center, New Mexico Institute of Mining and Technology, Socorro, New Mexico

(Manuscript received 5 August 2004, in final form 18 November 2004)

ABSTRACT

The lightning data that are recorded with a three-dimensional lightning mapping array (LMA) are compared with data from an electric field change sensor (in this case a flat-plate antenna operated both as a "slow" and a "fast" antenna). The goal of these comparisons is to quantify any time difference that may exist between the initial responses of the two instruments to a lightning flash. The data consist of 136 flashes from two New Mexico thunderstorms. It is found that the initial radiation source detected by the LMA usually precedes the initial response of both the slow and fast antennas. In a small number of cases, the flat-plate antenna response precedes the initial LMA source, but by no more than 2 ms. The observations of such a close time coincidence suggest that the first LMA radiation source of each flash was located at or very near the flash-initiation point. Thus, the first LMA radiation source and the initial sequence of sources from a lightning flash can be used as remote sensing tools to give information about the magnitude of the electric field (relative to lightning-initiation thresholds) and the direction of the electric field at the initiation location.

1. Introduction

Because charges are accelerated in a developing lightning flash, lightning emits electromagnetic radiation across a broad range of frequencies. This radiation can be used to determine the path of the flash through a thundercloud. The two main techniques for mapping the lightning's path have been time of arrival (TOA; e.g., Proctor 1971, 1981; Lennon 1975; Maier et al. 1995), using the very high frequency (VHF) portion of the radiation spectrum, and interferometry, using VHF radiation (e.g., Warwick et al. 1979; Richard et al. 1986; Rhodes et al. 1994; Shao and Krehbiel 1996). In this study we concentrate on lightning paths determined with the lightning mapping array (LMA; Rison et al. 1999). The LMA detects VHF radiation and uses a TOA technique that is conceptually similar to the one developed by Lennon (1975).

As a flash develops, the in-cloud electric field vector $\mathbf{E}_c$ influences its path. However, it is generally difficult to determine $\mathbf{E}_c$ from the path of the flash because once the flash has developed a substantial length, it will perturb the local field. In a few situations the magnitude and/or the direction of $\mathbf{E}_c$ can be determined. For instance, extensive horizontal branches occur approximately at the altitudes of potential wells (Coleman et al. 2003), and these wells occur where the vertical component of $\mathbf{E}_c$ is zero. In this paper, we first describe how the initiation point of a flash is another location along the lightning path where the direction and the relative magnitude of $\mathbf{E}_c$ can be determined. The central part of

Corresponding author address: Chris Maggio, Department of Physics and Astronomy, 108 Lewis Hall, University of Mississippi, Post Office Box 1848, University, MS 38677-1848.
E-mail: crmaggio@hotmail.com

the paper is then devoted to showing whether the first radiation sources that are detected by the LMA are close to the flash-initiation location.

2. Lightning initiation

A lightning flash is initiated (presumably) when a spark occurs at a location in the cloud where there is a large $\mathbf{E}_c$ magnitude; the flash then extends away from this initiation location. Exactly how large $\mathbf{E}_c$ is at the initiation location depends on several factors, including the type of breakdown, the altitude of the initiation (because the breakdown field depends on molecular spacing, which depends on altitude), and, perhaps, on the type and shape of local hydrometeors, which can enhance $\mathbf{E}_c$ locally (e.g., Crabb and Latham 1974; Griffiths and Latham 1974b). Several different methods for lightning initiation have been proposed: conventional dielectric breakdown, conventional dielectric breakdown enhanced by hydrometeors, and runaway breakdown of energetic (~1 MeV) electrons. Conventional breakdown occurs at approximately 3 MV m^{-1} at 1 atm pressure (MacGorman and Rust 1998, p. 15). Conventional breakdown enhanced by hydrometeors can occur in fields in the 400–500 kV m^{-1} range for corona discharge from the surface of ice hydrometeors (e.g., Griffiths and Latham 1974a; Griffiths 1975; Latham and Stromberg 1977), and in fields as low as 350 kV m^{-1} for corona discharge from colliding raindrops (e.g., Crabb and Latham 1974; Latham and Stromberg 1977). Theoretical calculations indicate that runaway breakdown initiation can occur above field thresholds of 75–105 (Gurevich and Zybin 2001) or 100–140 (Dwyer 2003) kV m^{-1} in the altitude range descending from 9–6 km. Therefore, the $\mathbf{E}_c$ magnitude at the flash-initiation location is presumably as large as the smallest of these threshold values or larger.

Kasemir (1960) suggested that after the initial spark starts a lightning flash, a bidirectional leader propagates away from the initiation location. This leader is net neutral, but has opposite polarity charges at its two ends (as well as distributed along the length of the leader). Bidirectional leaders have been observed for lightning flashes triggered by aircraft inside thunderstorms (e.g., Mazur 1989; Kawasaki et al. 2002) and have been inferred for other flashes (e.g., Kawasaki et al. 2002). It is likely that $\mathbf{E}_c$ controls the behavior of the flash immediately after initiation because $\mathbf{E}_c$ is not (yet) perturbed by the electric field of the leader ($\mathbf{E} = \mathbf{E}_c$ at initiation, but after a substantial leader develops, $\mathbf{E} = \mathbf{E}_c + \mathbf{E}_l$, where $\mathbf{E}_l$ is the field due to the leader charges). This fact allows us to determine the direction of $\mathbf{E}_c$ at the flash-initiation location—the $\mathbf{E}_c$ vector points in the opposite (same) direction of the propagation direction of the detected negative (positive) polarity breakdown.

The LMA locates sources of impulsive VHF radiation in the 60–66-MHz band by measuring the arrival times of the radiation at six or more receiving stations in an array of eight (or more) stations (Rison et al. 1999; Thomas et al. 2004). The time and magnitude of the peak radiation event during each 80–100-μs time interval of the flash are recorded at each station. Events detected at six or more stations are located in three spatial dimensions and in time. In this article, we refer to radiation peaks that are detected and located by the LMA as radiation sources or events. Each radiation source is characterized by its position, time, peak source power, and the goodness-of-fit chi-squared (χ^2_ν) value of the location results. For our study we chose a goodness-of-fit value of 5 for all accepted LMA data.

Using the LMA, it is possible to distinguish between the two ends of the leader, because they radiate differently in the VHF (e.g., Shao and Krehbiel 1996; Rison et al. 1999). In particular, negative polarity breakdown is a more copious producer of impulsive breakdowns in the VHF than positive polarity breakdown (Rison et al. 1999). In addition, Thomas et al. (2001) found that the more powerful LMA sources from a lightning flash are usually associated with negative polarity breakdown. For these reasons, it is possible to use the LMA data to determine the direction of the local $\mathbf{E}_c$ vector as the leader first begins to propagate away from the flash-initiation location.

Thus, for any flash, the first sources detected by the LMA will give information about the relative magnitude and direction of the electric field at the lightning-initiation location if these first sources are close in time and space to the initiation. Our main goal then is to quantify how well the first LMA radiation sources represent a flash's initiation location.

3. Instrumentation and analysis approach

The data were collected as part of an experiment called A Study of Electrical Evolution in Thunderstorms (SEET; Coleman et al. 2003). SEET was conducted in July and August of 1999 to study mountain thunderstorms at Langmuir Laboratory in central New Mexico. Three-dimensional maps of individual lightning flashes were obtained with the LMA. A flat-plate antenna (operated as an electric field change sensor) measured "slow" (10-s decay time constant) and "fast" (100-μs decay time constant) electric field changes of the flashes (Kitagawa and Brook 1960). A series of balloons, each carrying an electric field meter (Winn et al. 1978; Marshall et al. 1995) and a GPS radiosonde

(Hock and Franklin 1999; Coleman et al. 2003), were flown into several thunderstorms occurring above the laboratory. In addition, radar data of the storms were collected with two radars.

We compare the timing of the initial response of both the LMA and the flat-plate antenna to a lightning flash to determine if the first source of radiation located by the LMA occurs before or after the flat-plate antenna response. In a few cases, balloons carrying electric field meters were relatively close to the initial LMA radiation source of a flash; for these cases we compare the in situ **E** measurements to the inferred $\mathbf{E}_c$ direction and large magnitude. Shao and Krehbiel (1996) showed that the initial VHF radiation (at 274 MHz) from lightning flashes preceded the response of the flat-plate antenna. Our test will determine if this is also true in the 60–66-MHz band, and, more importantly, if the radiation is impulsive enough to allow for an LMA source to be detected close to the flash initiation. For the comparison of LMA and slow antenna data, we consider the following two possible scenarios.

1) The first events of a flash are powerful enough to trigger the LMA before an appreciable charge is moved within the cloud. As a result, the initial response of the LMA to a lightning flash precedes the response of the slow antenna.
2) The initial charge motion is not impulsive enough to trigger the LMA; therefore, the initial response of the slow antenna to a lightning flash precedes the LMA's first source.

Because the LMA and the fast antenna both respond to impulsive radiation events, but at different frequencies, the comparison of LMA and fast antenna data investigates which instrument first detects the impulsive radiation events that occur during lightning initiation. Although this is primarily a question of relative signal amplitudes, sensitivities, and trigger levels, we need to determine, in particular, the relative timing of the first LMA source compared to the first fast antenna response.

We examined LMA data, slow antenna data, and fast antenna data for 136 lightning flashes on 2 August 1999; 74 flashes occurred between 2130:00 and 2239:59 UTC within the LMA perimeter (in particular, over the center of the network) and approximately 30 km from the flat-plate antenna, and 62 flashes occurred between 2102:01 and 2149:59 UTC closer to the flat-plate antenna and outside of the LMA perimeter. Figure 1 shows a detailed map of the locations of the LMA stations, flat-plate antenna, and LMA-recorded initiation sources for both sets of the flashes. Antenna versus LMA time delays were determined from a continuous

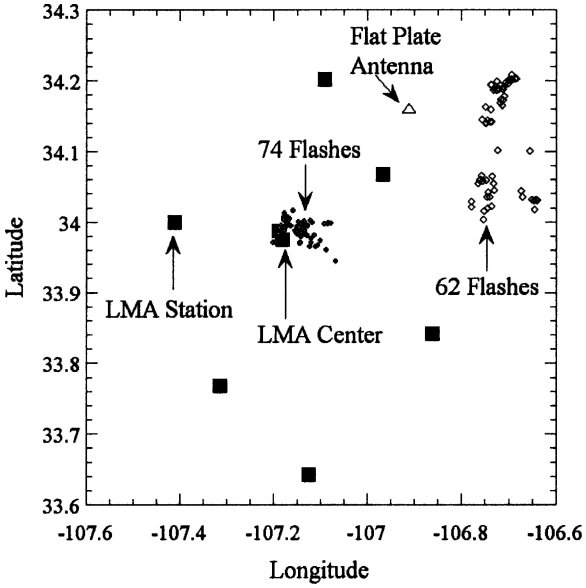

FIG. 1. Geographic locations of the LMA stations, flat-plate antenna, and LMA-recorded lightning-initiation sources for the group of 74 flashes within the LMA sensor perimeter, and for the group of 62 flashes outside the LMA perimeter. The center of the LMA network was approximately 30 km from the flat-plate antenna and approximately 45–50 km from the 62 flashes.

record of the slow antenna data and a triggered record of the fast antenna data (plotting electric field strength in volts per meter versus time) along with LMA data (plotting altitude versus time) for each individual flash. The LMA data on these graphs are represented by individual source locations, each occurring at some instant in time. Thomas et al. (2004) have shown that for flashes occurring within the perimeter of the network of the LMA sensors, the source locations carry an uncertainty of 6–12-m rms in the horizontal and 20–30-m rms in the vertical. For the flashes occurring outside of the LMA perimeter in this study, source locations have an uncertainty of approximately 140-m rms in the horizontal and 120-m rms in the vertical.

Plots of the slow antenna data carry with them a degree of subjectivity. Every slow antenna plot for the flashes occurring in the above-mentioned time frames have a point in time where a significant deviation (either in a positive- or negative-sloped direction) from a preflash condition is observed. It is this point of deviation where the antenna is definitely responding to the electric field changes due to a particular lightning flash. The degree of subjectivity arises when trying to determine the exact point of significant deviation, primarily because of the background noise that exists in the slow antenna output.

Plots of the fast antenna–triggered data are much less subjective in interpretation than the slow antenna plots.

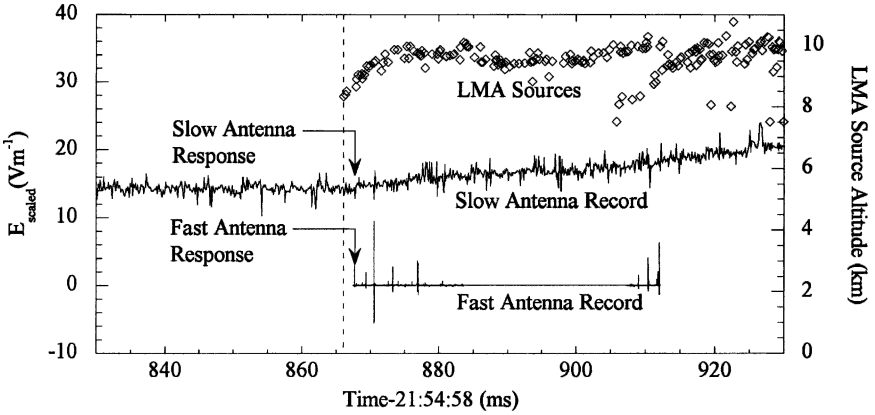

FIG. 2. An example of LMA, slow antenna, and fast antenna data during the initial part of an IC flash. The dashed line shows the time when the first LMA source was recorded, and the arrows highlight the first responses of the slow and fast antennas. For this flash, the LMA precedes the fast and slow antennas by approximately 1.6 ms.

Figure 2 shows a slow antenna, fast antenna, and LMA plot for a flash occurring at 2154:58 UTC. This example was chosen because it has a very distinct point of significant deviation in the slow antenna record. Fast antenna–triggered data on the plot appear in the form of individual impulsive events, or "spikes," at some instant in time. Figure 3 shows a slow antenna, fast antenna, and LMA plot for a flash occurring at 2147:17 UTC that also has a very distinct point of significant deviation in the slow antenna.

In this paper, a time delay is defined as the time between the first recorded source location by the LMA and either the point of significant deviation in the slow antenna plot or the point where the first spike occurs in the fast antenna plot. A positive time delay indicates that the first source that is recorded by the LMA precedes the point of significant deviation in the slow antenna or the point when the first spike occurs in the fast antenna. Likewise, a negative time delay indicates that either the slow or fast antenna response precedes the LMA.

One small detail in determining the response time of the flat-plate antenna and LMA to a lightning flash concerns propagation delays from the initiation event to the physical location of the instrument. The LMA radiation data are recorded at the various LMA stations, but the analysis determines when in time and space the impulsive event occurred. Based on the position uncertainties for the LMA sources mentioned above, the timing uncertainties were 0.1 μs for the 74

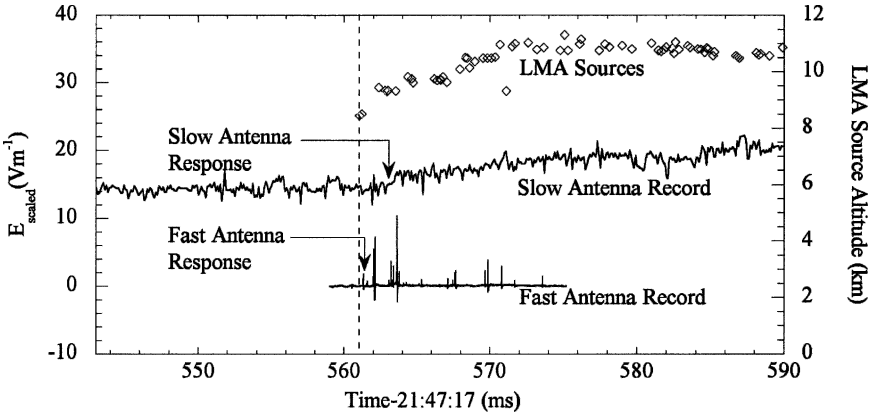

FIG. 3. An example of LMA, slow antenna, and fast antenna data during the initial part of a hybrid CG flash. The dashed line shows the time when the first LMA source was recorded and the arrows highlight the first responses of the slow and fast antennas. For this flash, the LMA precedes the slow antenna by approximately 2.3 ms and the fast antenna by approximately 0.2 ms.

flashes that occurred near the center of the LMA and 0.6 μs for the 62 flashes that occurred outside of the LMA sensor perimeter. The plots of flat-plate antenna data (i.e., in Figs. 2 and 3) have not been corrected for the time delay of the signal in reaching the antenna. The flat-plate antenna was located approximately 30 km away from the group of 74 flashes, and approximately 15–20 km from the group of 62 flashes, so there is a systematic delay between 0.05 and 0.10 ms for the flashes farthest away from the antenna. Reported response times between the LMA and flat-plate antenna have been adjusted for the propagation delay.

4. LMA versus slow and fast antenna time delay for flashes occurring within the LMA perimeter

Of the 74 flashes that occurred over the center of the LMA network, 51 were found to have a positive time delay of greater than 3 ms between the first recorded LMA source and the point of significant deviation in the slow antenna. Of the 23 remaining flashes, 19 exhibited a time delay that was positive, but less than 3 ms, and 4 exhibited a negative time delay where the first LMA source lagged the slow antenna response to a lightning flash. For these four flashes, the maximum slow antenna lead time over the LMA was approximately 1.7 ms.

From the plots of the triggered fast antenna data, 37 flashes were observed to have either a positive time delay of greater than 3 ms or no fast antenna activity that was strong enough to trigger a recording at the time of flash initiation. Of the 37 remaining flashes, 28 exhibited a time delay that was positive, but less than 3 ms, and 9 exhibited a negative time delay where the LMA source lagged the fast antenna response to the lightning flash. For these nine flashes, the maximum fast antenna lead time over the LMA was approximately 1.7 ms.

Our results show that the LMA precedes the slow antenna for 95% of the 74 flashes and precedes the fast antenna for 88% of the 74 flashes. No physical differences in the behavior of the flashes where the LMA preceded the flat-plate antenna were noted when compared to flashes where the antenna preceded the LMA. Therefore, in most cases, the LMA is responding to the event that initiates a lightning flash before the flat-plate antenna responds to the event. This suggests that the first LMA radiation source of each flash was located at or very near the flash-initiation point. Two reasons may explain the few cases in which the flat-plate antenna response preceded the LMA response. First, Thomas et al. (2004) have shown that local noise sources near the LMA stations sometimes interfere with the reception of impulsive event radiation so that the initial LMA source (or sources) is (are) missing. Second, spikes in the fast antenna data sometimes may be due to coincident flashes in other storms; these "extra" spikes can occur before the spikes from the flashes that are detected by the LMA, which can affect the time delay measurement between the LMA and fast antenna. Recently, Behnke et al. (2003) showed that lightning leader speeds range between 4×10^4 and 2×10^5 m s^{-1}. Multiplying our maximum negative time delay (1.7 ms) by the maximum leader speed, we get a maximum distance of 340 m. Thus, for the small number of cases where the LMA lags the flat-plate antenna, 340 m is the maximum distance between the first LMA source and the event that was first seen by the flat-plate antenna.

5. LMA versus slow and fast antenna time delay for flashes occurring outside the LMA perimeter

Geographically, SEET was focused on flashes that occurred within the perimeter of the LMA stations. However, the flat-plate antenna was located approximately 30 km northeast of the center of the LMA and outside the network perimeter. Because the antenna should be more sensitive to flashes occurring nearer to it, we studied 62 flashes from another thunderstorm on 2 August 1999, which occurred approximately 15–20 km from the flat-plate antenna. We wanted to be sure that the result of the LMA response leading the antenna response was not due to insensitivity of the antenna. Of the 62 flashes studied, 21% of them occurred within the same time interval as the 74 flashes discussed previously. The results for the 62 flashes were similar to the previous results, with the LMA leading the antenna's response most of the time—the LMA preceded the slow antenna for 86% of the 62 flashes, and preceded the fast antenna for 66% of the flashes. Again, we found that for the few cases when the antenna led the LMA, the antenna's lead time was not greater than 1.7 ms; in this case the maximum was 1.2 ms.

For the 62 flashes, however, the percentage in which the LMA leads the antenna is not as dominant as in the results for the 74 flashes. To better understand this difference, histograms of power values determined by the LMA for both sets of flashes were examined for the first 40 sources of each flash and are shown in Fig. 4. We denote the original set of 74 flashes as set 1 (centered within the LMA network) and the set of 62 flashes as set 2 (located outside of the LMA sensor perimeter and closer to the flat-plate antenna).

The histograms in Fig. 4 show that the LMA tended to not detect the lower-power sources (less than about

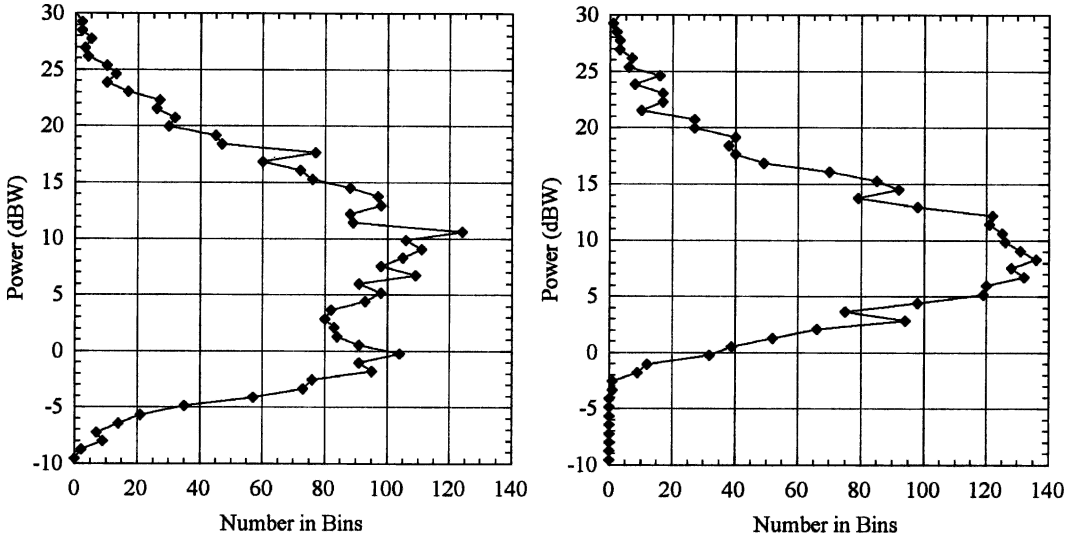

FIG. 4. Histogram for the power values of the first 40 LMA sources for (left) the set of 74 flashes and for (right) the set of 62 flashes. The bin size for both histograms is 0.777 dB.

5 dBW) for the flashes occurring outside the LMA perimeter. For higher-power sources (greater than 10 dBW), the histograms are similar. Based on the histograms in Fig. 4, we suspect that the LMA missed some initial sources with low power in set 2. If so, then this fact probably explains why there was a smaller percentage of LMA responses in set 2 leading the antenna responses than was seen in set 1. Figure 5 shows histograms of the power of the first LMA source of each flash for both sets. These histograms also indicate that the LMA detects lower-power initial sources for flashes centered in the LMA sensor network.

6. Electric fields within lightning-producing clouds

With our conclusions from the previous section that the LMA usually responds to a flash earlier than the flat-plate antenna, we expect the initial LMA source to occur in a relatively large $\mathbf{E}_c$ based upon the theoretical considerations of initiation mechanisms discussed in section 2. In situ electric field measurements can be used to verify the use of the LMA as a remote sensing tool to locate regions of strong electric fields in storms. Figures 6 and 7 show two examples of balloon $\mathbf{E}_c$ measurements made close to the initial LMA lightning

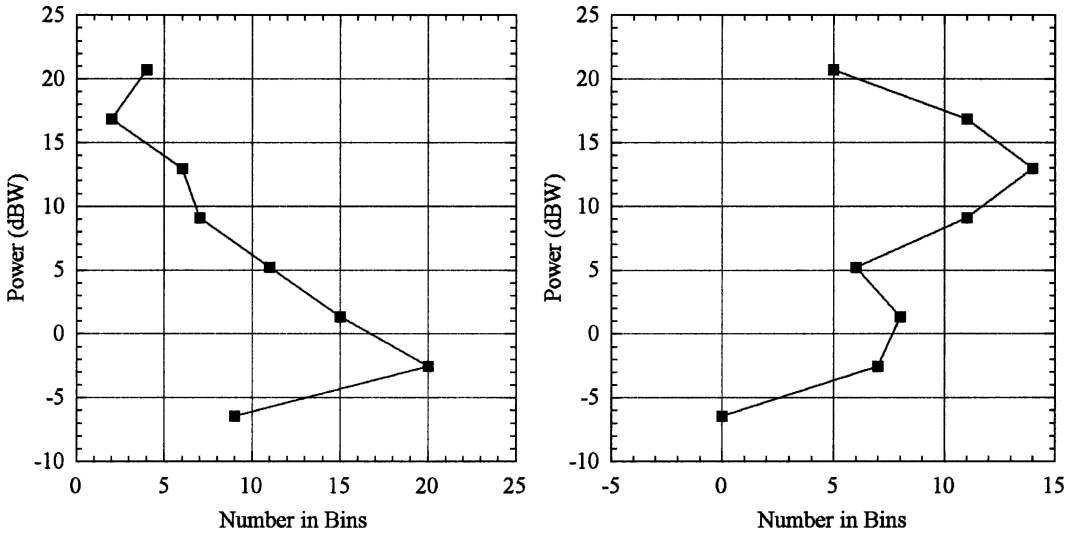

FIG. 5. Histogram of power values for the first source of each flash for (left) the set of 74 flashes and for (right) the set of 62 flashes. The bin size for both histograms is 3.882 dB.

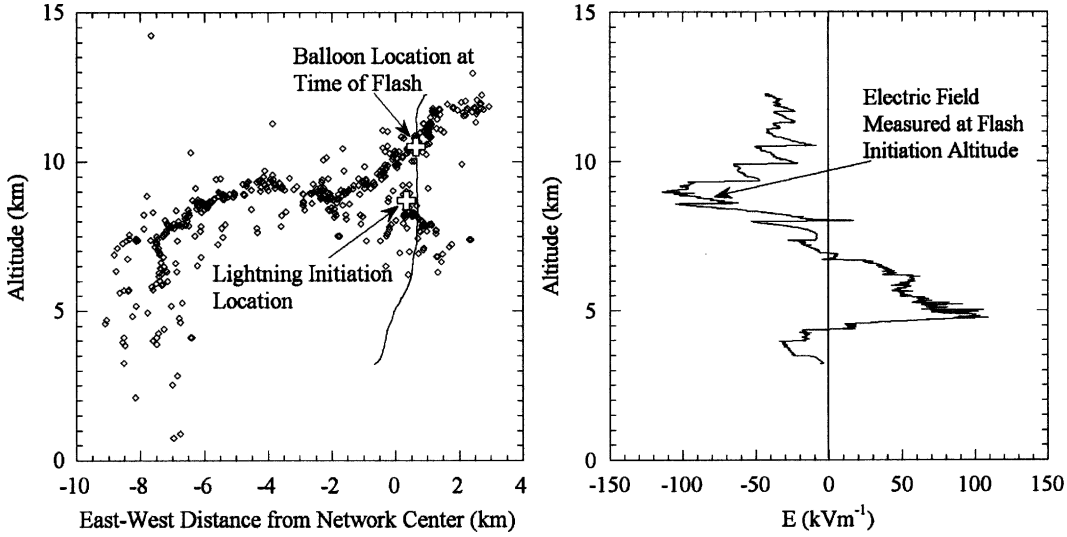

FIG. 6. (left) LMA sources for a hybrid CG flash at 2151:15 UTC on 2 Aug 1999 and balloon path overlay. The location of the initial LMA radiation source and the location of the balloon at the time of the flash are highlighted. (right) In the balloon ascent sounding, an electric field value of -81 kV m^{-1} was measured as the balloon ascended through the initiation altitude 137 s before the flash. At the time of the flash, the balloon was 1.8 km above, 1.0 km north, and 0.3 km east of the flash-initiation location.

source for two cloud-to-ground (CG) flashes. One of these flashes (Fig. 6) was a hybrid CG flash. A hybrid CG flash initiates above a negative charge region in the same manner as an intracloud (IC) flash, but it eventually goes to ground outside of the cloud. There was no balloon flight on 2 August that was close to the initiation of a CG flash, so a flash from 31 July has been used as the example in Fig. 7. The hybrid CG flash seen in Fig. 6 initiated at an altitude of 8.71 km and was near a balloon measurement of –81 kV m^{-1} that was taken 137 s before the flash. The CG flash in Fig. 7 initiated at an altitude of 5.73 km, 121 s after, and 40 m below, a

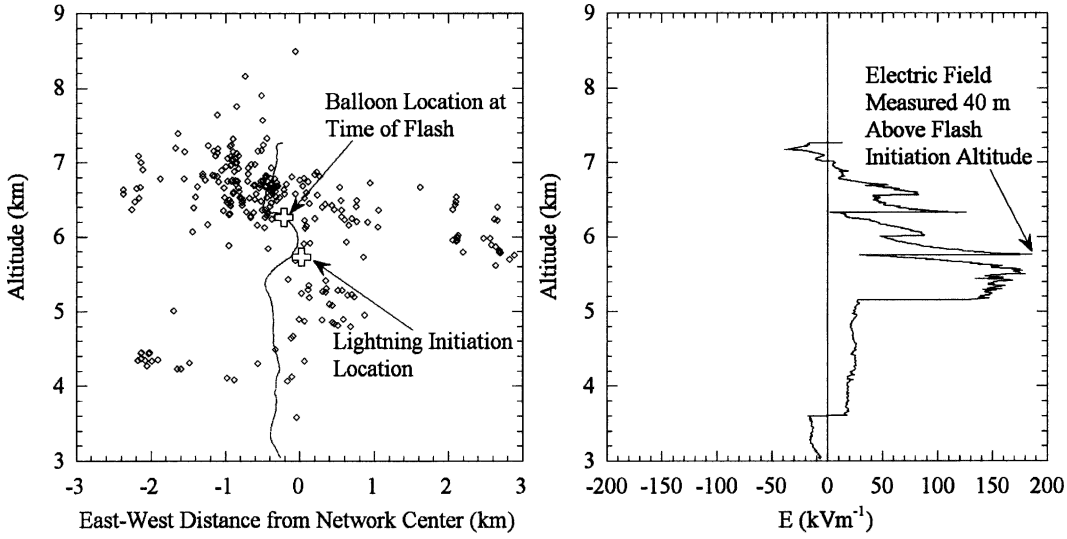

FIG. 7. (left) LMA sources of a CG flash at 2229:22 UTC on 31 Jul 1999 and balloon path overlay. The location of the initial LMA radiation source and the location of the balloon at the time of the flash are highlighted. (right) In the balloon descent sounding, an electric field value of 186 kV m^{-1} was measured as the balloon descended to within 40 m of the initiation altitude 121 s after the flash. At the time of the flash, the balloon was 0.5 km above, 0.1 km south, and 0.2 km west of the flash-initiation location.

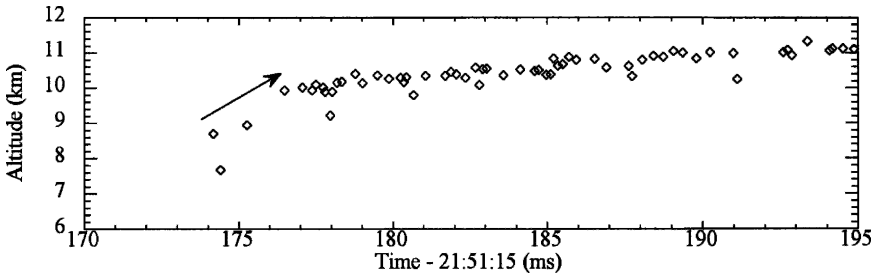

FIG. 8. LMA plot for the hybrid CG flash seen in Fig. 6. The arrow indicates the direction of negative polarity breakdown. The movement of negative charge to higher altitudes indicates a downward-pointing z component of the electric field vector. This is confirmed by the balloon sounding (Fig. 6) measuring an electric field near the flash-initiation location of -81 kV m^{-1}.

balloon measurement of $+186$ kV m^{-1} at an altitude of 5.77 km. These $\mathbf{E}_c$ values are considered "relatively large" in the sense that they are either close to or exceed the threshold for runaway breakdown at their respective altitudes. In Fig. 6 the $\mathbf{E}_c$ magnitude was 20% less than the Dwyer (2003) runaway breakdown threshold at a 8.71-km altitude, but was 4% more than the threshold of Gurevich and Zybin (2001). In Fig. 7 the $\mathbf{E}_c$ magnitude was 30% more than the Dwyer runaway breakdown threshold at a 5.77-km altitude, and was 70% more than the Gurevich and Zybin threshold.

The data in Fig. 6 and the associated LMA data suggest that the altitude region near 8.50 km was strongly electrified as the balloon ascended from 8.20 to 8.75 km. Three hybrid CG flashes and one IC flash initiated at altitudes of 8.20, 8.57, 8.65, and 8.71 km. The largest measured $\mathbf{E}_c$ was 105 kV m^{-1}, despite the repeated flashes in the vicinity of the balloon. The largest $\mathbf{E}_c$ values were approximately equal to the Dwyer threshold for runaway breakdown. Similarly, the flash-initiation data, combined with the balloon $\mathbf{E}_c$ data in Fig. 7, show that the balloon descended through a strongly electrified region of the cloud near a 5.77-km altitude (Marshall et al. 2005). These data provide further evidence for our hypothesis that the initial LMA source of a flash occurs at a location of a large electric field (relative to runaway breakdown thresholds).

In addition to being able to use LMA data to find regions of strong electric fields, the LMA can also provide information regarding the direction of $\mathbf{E}_c$. Because the LMA is a three-dimensional mapping instrument, it gives information about the flash-propagation direction and, hence, both the vertical and horizontal components of the electric field. As a simple example of this idea, we show how to determine the direction of the vertical component of the electric field vector $\mathbf{E}_z$, because this component is easily seen in the time–altitude LMA plots and is often the most significant component of $\mathbf{E}_c$ (Marshall and Rust 1991). Figures 8 and 9 show LMA data for the two flashes in Figs. 6 and 7. On these two LMA plots are arrows indicating the direction of propagation for the first several radiation sources of each flash. Figure 8 shows that the hybrid CG propagated initially upward in altitude, suggesting a negative electric field at the time and location of flash initiation. Figure 9 shows that the CG flash propagated initially downward in altitude, suggesting a positive electric

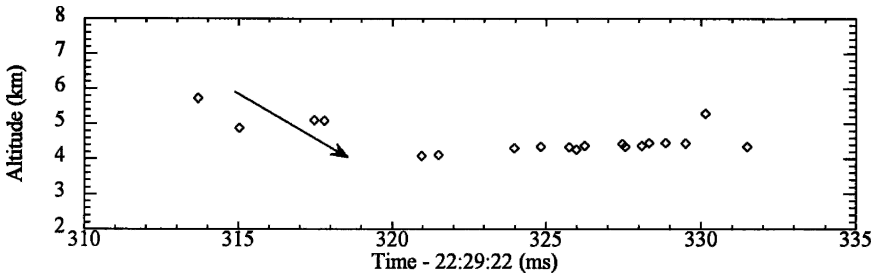

FIG. 9. LMA plot for the CG flash seen in Fig. 7. The arrow indicates the direction of negative polarity breakdown. The movement of negative charge to lower altitudes indicates an upward-pointing z component of the electric field vector. This is confirmed by the balloon sounding (Fig. 7) measuring an electric field near the flash-initiation location of 186 kV m^{-1}.

field at the time and location of flash initiation. The LMA-derived directions of the z component of the electric field vector are verified by the balloon measurements shown in Fig. 6 (upward motion of negative polarity breakdown compared to $\mathbf{E}_c$ of -81 kV m^{-1}) and in Fig. 7 (downward motion compared to $\mathbf{E}_c$ of $+186$ kV m^{-1}).

7. Conclusions

In our comparison of lightning data recorded with a three-dimensional LMA to data acquired with an electric field change sensor (in this case a flat-plate antenna operated both as a "slow" and a "fast" antenna), we have quantified the time difference that exists between the initial responses of these instruments to a lightning flash. From this study, we draw the following several conclusions.

1) The LMA response to a lightning flash precedes the flat-plate antenna for 95% of the 74 flashes that occurred within the LMA perimeter when compared to the slow antenna, and for 88% of the 74 flashes when compared to the fast antenna. This result suggests that for most flashes, the first events are powerful enough to be detected by the LMA before the flat-plate antenna responds. From this, we infer that the first LMA radiation source of a flash is within a few tens of meters or less of the flash-initiation location.
2) The LMA response to a lightning flash precedes the slow antenna for 86% of the 62 flashes that occurred outside the LMA perimeter and closer to the flat-plate antenna (about 45–50 km from the center of the network), and for 66% of the 62 flashes when compared to the fast antenna. One possible reason for the LMA not leading the flat-plate antenna response for as large of a majority as for the group of 74 flashes occurring within the LMA network is that the lower-power initial sources (less than about 5 dBW) are not always detected for flashes that occur outside of the LMA perimeter.
3) In the few cases where the LMA lags the antenna response to a flash, the LMA is found to lag by less than 1.7 ms. For these cases, the breakdown was either not impulsive enough or not strong enough to be detected immediately by the LMA, impulsive events may have been preempted by local station noise, or distant lightning flashes may have "polluted" the fast antenna data. However, using typical propagation speeds, these flashes may have propagated only a few hundred meters before the LMA measured the impulsive radiation.
4) By using the LMA to locate in time and space the initiation of a lightning flash, we can infer this to be the location where strong electric fields should be present within clouds. In two cases of in situ balloon measurements of the electric field close to LMA-determined lightning-initiation locations, the measured electric field magnitudes were comparable to, or exceeded, the runaway breakdown thresholds of Gurevich and Zybin (2001) and Dwyer (2003).
5) The propagation direction of negative polarity breakdown is more easily detected by the LMA, because it is a more copious producer of impulsive breakdowns in the VHF (Rison et al. 1999). Because the LMA is capable of determining the direction of the negative breakdown, it can also determine the direction of the local electric field vector at flash initiation. Such inferences have been verified for the vertical component of the field in a few cases by balloon measurements.

In summary, we conclude that the first VHF radiation source that is detected by the LMA during a lightning flash provides a good indication of the flash-initiation location in space and time (at least for the region tested, namely, within 45–50 km of the center of the LMA array). Thus, the first LMA source can be used as a remote sensing tool to find the location of strong electric fields. As the lightning leader first begins to propagate away from the flash-initiation location, the direction of the local electric field vector is also remotely detected by the LMA.

Acknowledgments. This research was supported by NSF Grants ATM-0220842 and ATM-9912073.

REFERENCES

Behnke, S. A., R. J. Thomas, P. R. Krehbiel, and W. Rison, 2003: Propagation speeds of lightning leaders throughout an entire flash using 10μs time resolution 3D mapping data. *Eos, Trans. Amer. Geophys. Union,* **84** (Fall Meeting Suppl.), Abstract AE21A-1103.

Coleman, L. M., T. C. Marshall, M. Stolzenburg, T. Hamlin, P. R. Krehbiel, W. Rison, and R. J. Thomas, 2003: Effects of charge and electrostatic potential on lightning propagation. *J. Geophys. Res.,* **108,** 4298, doi:10.1029/2002JD002718.

Crabb, J. A., and J. Latham, 1974: Corona from colliding drops as a possible mechanism for the triggering of lightning. *Quart. J. Roy. Meteor. Soc.,* **100,** 191–202.

Dwyer, J. R., 2003: A fundamental limit on electric fields in air. *Geophys. Res. Lett.,* **30,** 2055, doi:10.1029/2003GL017781.

Griffiths, R. F., 1975: The initiation of corona discharges from charged ice particles in an electric field. *J. Electrost.,* **1,** 3–13.

——, and J. Latham, 1974a: A new method for the measurement of the surface electrical conductivity of ice. *J. Meteor. Soc. Japan,* **52,** 238–242.

——, and ——, 1974b: Electrical corona from ice hydrometeors. *Quart. J. Roy. Meteor. Soc.,* **100,** 163–180.

Gurevich, A. V., and K. P. Zybin, 2001: Runaway breakdown and electric discharges in thunderstorms. *Phys.-Uspekhi,* **44,** 1119–1140.

Hock, T. F., and J. L. Franklin, 1999: The NCAR GPS dropwindsonde. *Bull. Amer. Meteor. Soc.,* **80,** 407–420.

Kasemir, H. W., 1960: A contribution to the electrostatic theory of a lightning discharge. *J. Geophys. Res.,* **65,** 1873–1878.

Kawasaki, Z., S. Yoshihashi, and L. Jong Ho, 2002: Verification of Bi-directional Leader Concept by interferometer observations. *J. Atmos. Electr.,* **22,** 55–79.

Kitagawa, N., and M. Brook, 1960: A comparison of intracloud and cloud-to-ground lightning discharges. *J. Geophys. Res.,* **65,** 1189–1201.

Latham, J., and I. M. Stromberg, 1977: Point-discharge. *Lightning*, R. H. Golde, Ed., Academic Press, 99–117.

Lennon, C. L., 1975: LDAR—A new lightning detection and ranging system. *Eos, Trans. Amer. Geophys. Union,* **56,** 991.

MacGorman, D. R., and W. D. Rust, 1998: *The Electrical Nature of Storms*. Oxford University Press, 422 pp.

Maier, L., C. Lennon, T. Britt, and S. Schaefer, 1995: Lightning Detection and Ranging (LDAR) System performance analysis. Preprints, *Sixth Conf. on Aviation Weather Systems,* Dallas, TX, Amer. Meteor. Soc., 305–309.

Marshall, T. C., and W. D. Rust, 1991: Electric field soundings through thunderstorms. *J. Geophys. Res.,* **96,** 22 297–22 306.

——, W. Rison, W. D. Rust, M. Stolzenburg, J. C. Willett, and W. P. Winn, 1995: Rocket and balloon observations of electric field in two thunderstorms. *J. Geophys. Res.,* **100,** 20 815–20 828.

——, M. Stolzenburg, C. R. Maggio, L. M. Coleman, P. R. Krehbiel, T. Hamlin, R. J. Thomas, and W. Rison, 2005: Observed electric fields associated with lightning initiation. *Geophys. Res. Lett.,* **32,** L03813, doi:10.1029/2004GL021802.

Mazur, V., 1989: Triggered lightning strikes to aircraft and natural intracloud discharges. *J. Geophys. Res.,* **94,** 3311–3325.

Proctor, D. E., 1971: A hyperbolic system for obtaining VHF radio pictures of lightning. *J. Geophys. Res.,* **76,** 1478–1489.

——, 1981: VHF radio pictures of cloud flashes. *J. Geophys. Res.,* **86,** 4041–4071.

Rhodes, C. T., X. M. Shao, P. R. Krehbiel, R. J. Thomas, and C. O. Hayenga, 1994: Observations of lightning phenomena using radio interferometry. *J. Geophys. Res.,* **99,** 13 059–13 082.

Richard, P., A. Delannoy, G. Labaune, and P. Laroche, 1986: Results of spatial and temporal characterization of the VHF-UHF radiation of lightning. *J. Geophys. Res.,* **91,** 1248–1260.

Rison, W., R. J. Thomas, P. R. Krehbiel, T. Hamlin, and J. Harlin, 1999: A GPS-based three-dimensional lightning mapping system: Initial observations in central New Mexico. *Geophys. Res. Lett.,* **26,** 3573–3576.

Shao, X. M., and P. R. Krehbiel, 1996: The spatial and temporal development of intracloud lightning. *J. Geophys. Res.,* **101,** 26 641–26 668.

Thomas, R. J., P. R. Krehbiel, W. Rison, T. Hamlin, J. Harlin, and D. Shown, 2001: Observations of VHF source powers radiated by lightning. *Geophys. Res. Lett.,* **28,** 143–146.

——, ——, ——, S. J. Hunyady, W. P. Winn, T. Hamlin, and J. Harlin, 2004: Accuracy of the Lightning Mapping Array. *J. Geophys. Res.,* **109,** D14207, doi:10.1029/2004JD004549.

Warwick, J. W., C. O. Hayenga, and J. W. Brosnahana, 1979: Interferometric directions of lightning sources at 34 MHz. *J. Geophys. Res.,* **84** (C5), 2457–2468.

Winn, W. P., C. B. Moore, C. R. Holmes, and L. G. Byerley III, 1978: A thunderstorm of July 16, 1975, over Langmuir Laboratory: A case study. *J. Geophys. Res.,* **83,** 3080–3092.